

SUPPORTING MATERIAL

Source apportionment of fine particulate matter over the Eastern U.S. Part II: source apportionment simulations using CAMx/PSAT and comparisons with CMAQ source sensitivity simulations

Michael Burr, Yang Zhang

Department of Marine, Earth, and Atmospheric Sciences, North Carolina State University, Raleigh, NC, 27695

CONTENT

CAMx Model Evaluation and Comparison with CMAQ

Figure S1. Monthly-mean absolute difference in the wet deposition fluxes of NH_4^+ , NO_3^- , and SO_4^{2-} from CMAQ and CAMx (i.e., CAMx – CMAQ) in January and July.

Figure S2. Spatial distribution monthly-mean concentrations of max 8-hr O_3 (top) and 24-hr average $\text{PM}_{2.5}$ simulated by CAMx overlaid with observations from AIRS-AQS, IMPROVE, STN, and SEARCH in January and July.

Table S1. Performance statistics for surface concentrations of $\text{PM}_{2.5}$ components simulated by CAMx in January 2002

Table S2. Performance statistics for surface concentrations of $\text{PM}_{2.5}$ components simulated by CAMx in July 2002

CAMx Model Evaluation and Comparison with CMAQ

Tables S1 and S2 show evaluation of the wet deposition fluxes of SO_4^{2-} , NO_3^- , and SO_4^{2-} from CAMx in January and July (similar evaluation for CMAQ can be found in Tables S-2 and S-3 of Part I). CAMx underpredicts the wet deposition fluxes of SO_4^{2-} , NO_3^- , and NH_4^+ in January with NMBs of -68.8%, -96.4%, and -82.0%, respectively. CAMx overpredicts the wet deposition flux of SO_4^{2-} in July with an NMB of 21.6% and underpredicts the wet deposition flux of NO_3^- and NH_4^+ with NMBs of -99.6% and -47.0%, respectively. CMAQ performs significantly better for all 3 species in January, with NMBs of -20.3% to 1.3%. Both models overpredict the wet deposition flux of SO_4^{2-} and underpredict those of NO_3^- and NH_4^+ in July, though CMAQ performs slightly better. The MNB and MNE statistical measures are not applicable for wet deposition fluxes due to several hourly observations with no precipitation. Figure S1 shows the absolute difference (i.e., CAMx – CMAQ) in the wet deposition fluxes of NH_4^+ , NO_3^- , and SO_4^{2-} in January and July. The difference plots are consistent with the statistical analysis shown in Tables S2 and S3 in Part I and Tables S1 and S2 in Part II, with CMAQ predicting higher wet deposition of NO_3^- and NH_4^+ in January and July and SO_4^{2-} in January while CAMx predicts higher wet deposition of SO_4^{2-} in July. The differences in wet deposition fluxes between the two models may be explained by differences in wet deposition treatments between the two models, in addition to differences in the vertical mixing that causes different gas- and aqueous-phase concentrations for depositing species. In CMAQ, at a horizontal grid spacing of greater than 8-km, sub-grid size clouds are treated in addition to completely-resolved clouds. Conversely, in CAMx, aqueous-phase chemistry is treated only in resolved clouds that encompass the entire grid cell (Byun and Schere, 2006). This difference in number of clouds

treated may explain larger wet deposition fluxes of NO_3^- and NH_4^+ in January and July and SO_4^{2-} in January. The higher wet deposition of SO_4^{2-} from CAMx in July may also be related to differences in wet deposition treatments for PM with different sizes. In CMAQ, all accumulation and coarse mode particles within a cloud are completely absorbed while nuclei mode particles are slowly scavenged. Conversely, all PM mass within a cloud is assumed to be in the cloud water by CAMx (ENVIRON, 2009), possibly explaining the higher wet deposition flux of SO_4^{2-} by CAMx in July.

Figure S2 shows the spatial distribution of simulated monthly-mean max 8-h average O_3 by CAMx overlaid with observations from AIRS-AQS, CASTNET, and SEARCH in January and July, respectively. CMAQ (see Figure S1 in Part I) and CAMx predict similar spatial distribution of O_3 in January, with higher concentrations across the southern half of the domain. Both models perform reasonably well in reproducing observations, though CAMx shows a slight overprediction of O_3 across the Gulf States. CAMx predicts higher O_3 throughout the domain in July. CAMx performs better across the upper Midwest in July, while CMAQ performs slightly better across the Mid-Atlantic States.

Figure S2 also shows the spatial distribution of simulated monthly-mean $\text{PM}_{2.5}$ by CAMx overlaid with observations from IMPROVE, SEARCH, STN, and AIRS-AQS in January and July, respectively; which can be compared to Figure S1 for CMAQ in Part I. Both models show similar spatial distribution, capturing the general spatial distribution throughout the Mid-Atlantic States in January, though they overpredict in the Atlanta area and the northeast U.S., possibly due to overestimation of emissions of gaseous PM precursors in urban areas (Zhang et al., 2006). The majority of the upper-Midwest shows an overprediction, with the exception of Chicago and St. Louis, where underpredictions occur. In July, both models consistently underpredict $\text{PM}_{2.5}$ across the entire domain, possibly due to the overestimation of precipitation in July (Burr and Zhang, 2010).

Table S1. Performance statistics for surface concentrations of PM_{2.5} components simulated by CAMx in January 2002

Variable	Network	January								
		MeanObs	MeanSim	Number	NMB	NME	MNB	MNE	RMSE	COR
24-h avg. SO ₄ ²⁻	CASTNET	2.5	2.4	173	-5.6	27.4	-2.5	27.4	0.8	39.6
	IMPROVE	2.4	2.8	292	17.2	44.4	23.2	46.1	1.7	67.7
	SEARCH	2.2	3.7	1 334	68.7	99.3	218.4	239.1	3.4	13.6
	STN	3.4	3.1	645	-8.7	48.1	66.8	102.1	2.9	28.7
	AIRS-AQS	2.9	2.9	625	3.2	36.7	68.8	96.9	1.5	61.8
24-h avg. NO ₃ ⁻	CASTNET	2.3	1.7	173	-24.6	49.7	2.3	70.9	1.1	70.6
	IMPROVE	1.5	1.3	292	-11.4	53.8	-10.6	72.7	1.2	72.9
	SEARCH	1.7	1.7	1 319	1.4	91.7	161.1	241.6	2.3	18.7
	STN	3.7	3.3	565	-9.4	57.8	10.3	71.4	2.1	47.1
	AIRS-AQS	3.1	3.1	545	-1.6	49.3	5.4	64.3	2.2	36.4
24-h avg. NH ₄ ⁺	CASTNET	1.3	1.2	173	-8.6	25.4	1.4	29.3	41.4	73.5
	SEARCH	0.9	1.5	822	58.1	86.4	358.3	370.2	1.1	26.7
	STN	2.2	1.9	646	-12.4	58.7	120.4	151.3	2.6	28.6
	AIRS-AQS	1.6	1.8	626	13.7	40.3	Inf	Inf	0.9	63.7
24-h avg. BC	IMPROVE	0.4	0.4	294	3.6	42.7	9.7	41.3	0.4	51.8
	SEARCH	1.5	2.4	743	58.4	1.2	202.3	224.1	2.4	15.6
24-h avg. OC	IMPROVE	2.3	1.6	294	-1.5	45.7	13.4	48.7	1.2	52.1
	SEARCH	3.4	3.5	62	3.1	35.6	21.3	46.8	1.5	71.4
24-h avg. TC	SEARCH	5.4	5.5	1 132	1.0	66.6	96.6	136.2	4.1	32.7
	STN	5.3	3.9	633	-25.9	54.5	24.8	86.8	4.3	27.9
	IMPROVE	2.0	2.0	294	0.1	43.6	10.9	44.8	1.5	53.9
	AIRS-AQS	4.9	3.8	620	-22.2	47.4	3.4	64.0	3.4	32.5
SO ₄ ²⁻ _WD	NADP	1.3	0.4	335	-68.8	73.6	NaN	NaN	1.4	27.8
NO ₃ ⁻ _WD	NADP	1.6	0.1	335	-96.4	96.6	NaN	NaN	2.2	17.1
NH ₄ ⁺ _WD	NADP	0.3	0.1	335	-82.0	84.2	NaN	NaN	45.3	18.1

MeanObs: Mean Observed Values; MeanSim: Mean Simulated Values; NMB: Normalized Mean Bias; NME: Normalized Mean Error, MNB: Mean Normalized Bias; MNE: Mean Normalized Error; RMSE: Root Mean Square Error; COR: Correlation Coefficient; Inf: Infinity (which occurs when observed values are extremely small); NaN : Not a Number (which occurs when observed values are zero).

Table S2. Performance statistics for surface concentrations of PM_{2.5} components simulated by CAMx in July 2002

Variable	Network	July								
		MeanObs	MeanSim	Number	NMB	NME	MNB	MNE	RMSE	COR
24-h avg. SO ₄ ²⁻	CASTNET	7.3	6.7	183	8.7	20.4	-7.4	21.3	2.1	80.7
	IMPROVE	6.7	5.8	349	13.3	38.6	3.4	52.1	3.6	74.6
	SEARCH	5.9	8.0	986	35.4	87.1	237.1	268.4	7.5	17.2
	STN	7.7	6.3	1 016	-17.4	47.1	13.4	61.9	6.4	49.5
	AIRS-AQS	6.9	6.3	942	-8.3	34.2	16.3	52.9	3.3	81.4
24-h avg. NO ₃ ⁻	CASTNET	0.4	0.1	183	-84.9	92.3	-60.9	91.3	0.6	9.6
	IMPROVE	0.4	0.1	349	-85.6	94.3	-85.8	94.6	0.5	20.7
	SEARCH	0.6	0.2	1 444	-60.6	1.1	-38.9	130.3	1.3	8.4
	STN	2.2	0.2	938	-90.7	96.7	-74.2	95.8	6.2	1.4
	AIRS-AQS	0.9	0.2	864	-74.3	86.7	-77.3	91.1	99.6	41.4
24-h avg. NH ₄ ⁺	CASTNET	2.1	1.3	183	-40.8	43.7	-36.3	40.1	1.2	65.8
	SEARCH	2.1	1.8	1 412	-12.6	50.3	45.3	93.2	1.4	39.7
	STN	3.3	1.5	1 016	-52.5	64.2	29.3	92.9	5.8	20.3
	AIRS-AQS	2.2	1.6	942	-26.5	43.6	Inf	Inf	1.4	76.7
24-h avg. BC	IMPROVE	0.4	0.4	317	-4.6	66.7	Inf	Inf	0.5	49.7
	SEARCH	0.8	0.9	1 233	13.3	72.6	96.8	139.4	90.7	50.4
24-h avg. OC	IMPROVE	2.7	1.6	317	-39.4	62.4	-24.3	69.1	3.4	54.1
	SEARCH	3.4	2.5	62	-27.6	33.9	-24.8	32.1	1.4	71.4
24-h avg. TC	SEARCH	5.0	3.1	1 256	-39.6	51.2	-28.3	53.6	3.4	42.5
	STN	9.1	3.4	98	-58.7	70.6	-31.9	75.8	11.6	45.3
	IMPROVE	3.1	2.0	317	-34.7	61.5	-21.2	67.8	3.6	54.7
	AIRS-AQS	7.5	3.6	931	-51.7	61.6	-33.9	66.7	7.9	54.8
SO ₄ ²⁻ _WD	NADP	2.1	2.5	324	21.6	83.5	NaN	NaN	3.0	29.6
NO ₃ ⁻ _WD	NADP	1.7	0.0	324	-99.6	99.9	NaN	NaN	2.1	0.9
NH ₄ ⁺ _WD	NADP	0.4	0.2	324	-47.0	78.3	NaN	NaN	47.2	14.2

MeanObs: Mean Observed Values; MeanSim: Mean Simulated Values ; NMB: Normalized Mean Bias; NME: Normalized Mean Error, MNB: Mean Normalized Bias; MNE: Mean Normalized Error; RMSE: Root Mean Square Error; COR: Correlation Coefficient; Inf: Infinity; NaN : Not a Number

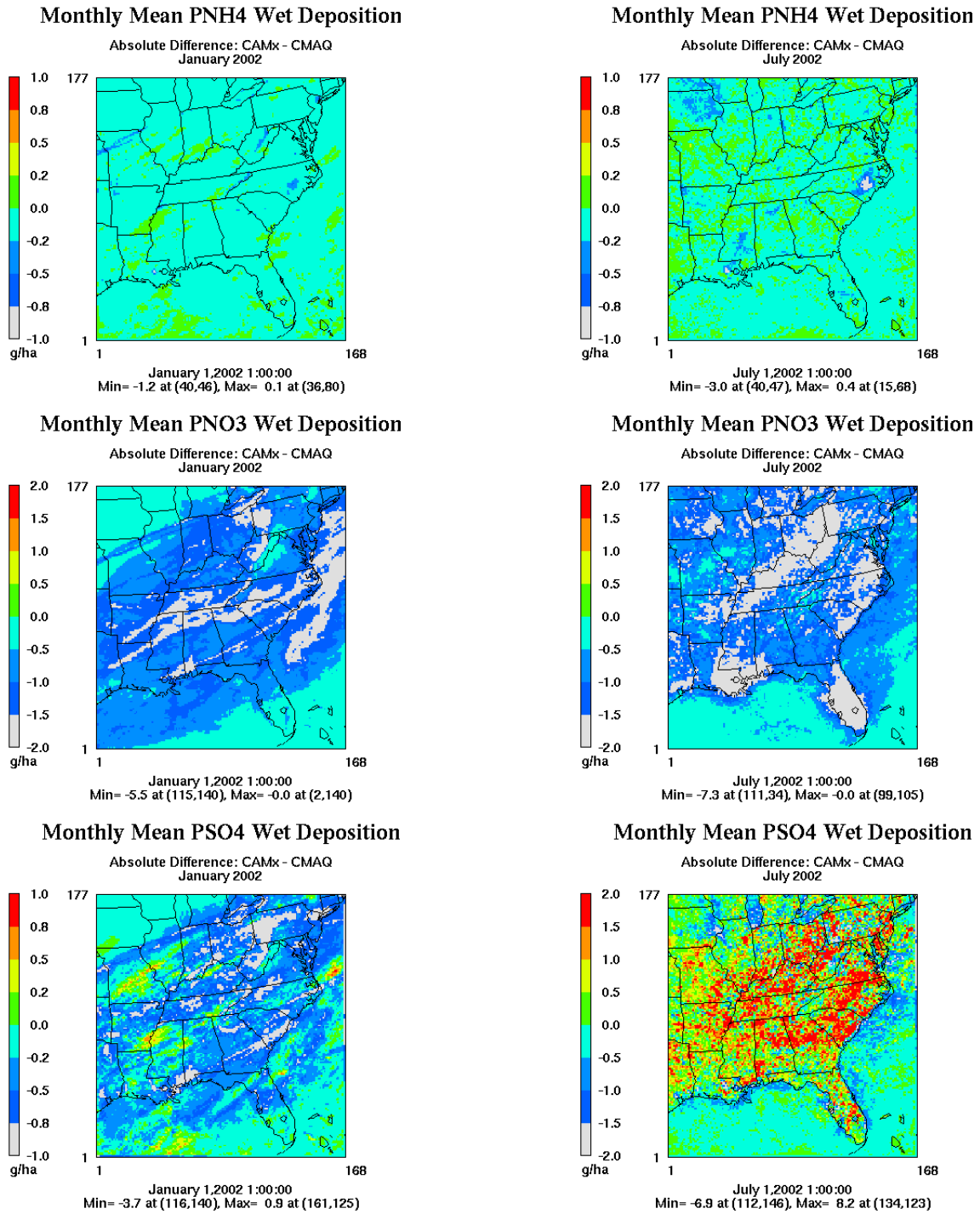


Figure S1. Monthly-mean absolute difference in the wet deposition fluxes of NH_4^+ , NO_3^- , and SO_4^{2-} from CMAQ and CAMx (i.e., CAMx - CMAQ) in January (left) and July (right).

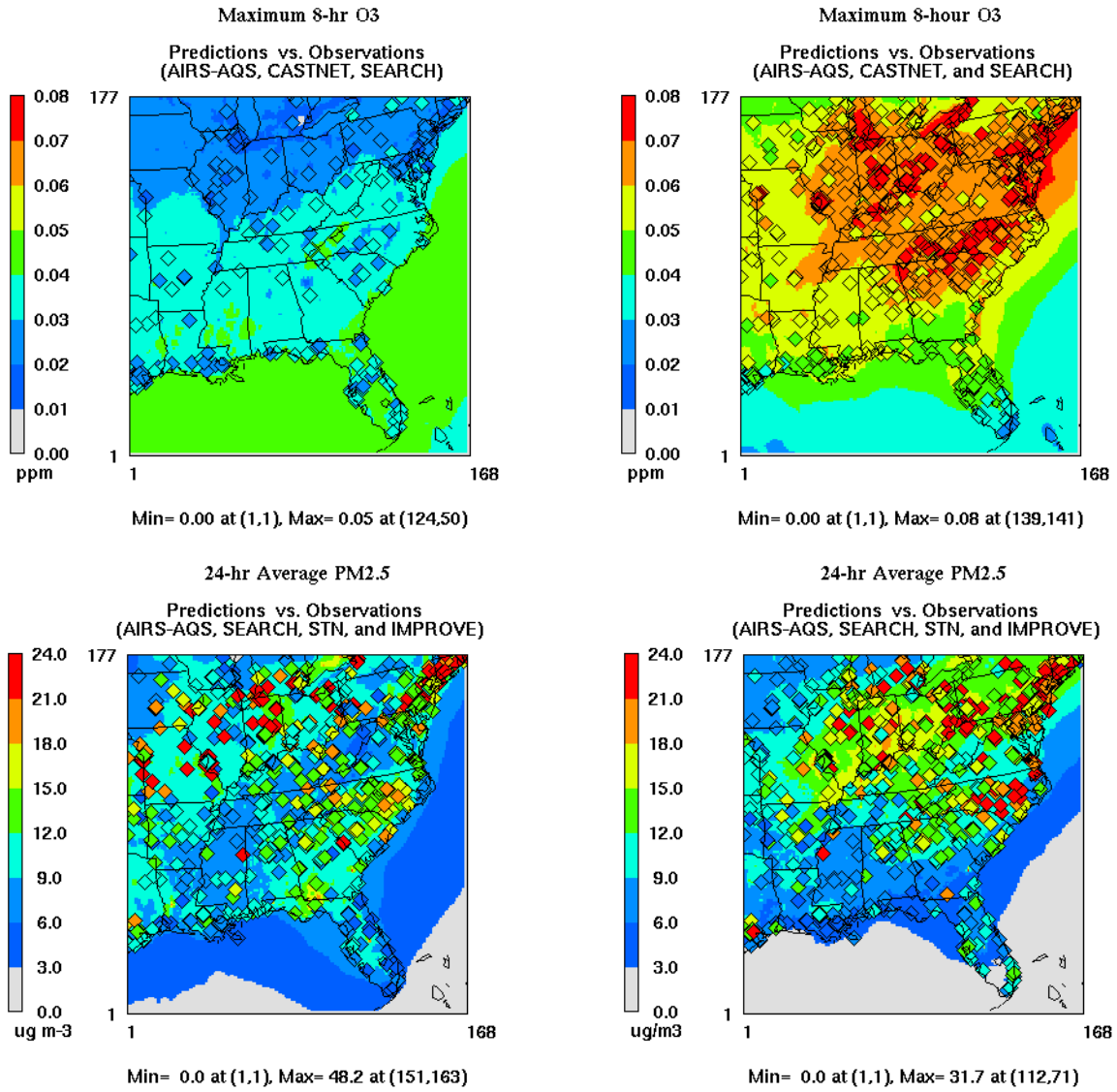


Figure S2. Spatial distribution monthly-mean concentrations of max 8-hr O₃ (top) and 24-hr average PM_{2.5} (bottom) simulated by CAMx overlaid with observations from AIRS-AQS, IMPROVE, STN, and SEARCH in January (left) and July (right).